J. Eng. Technol. Sci., Vol. 54, No. 1, 2022, 220111

Curie Point Depth Analysis of Lesugolo Area, East Nusa Tenggara, Indonesia Based on Ground Magnetic Data

Alamta Singarimbun[1], Umar Said[1], Dini Andriani[2], R.B. Astro[3], Bakrun[4], I G P.F. Soerya Djaja[1], Eleonora Agustine[5], Pepen Supendi[6,7] & Wahyu Srigutomo[1,*]

[1]Physics of Earth and Complex Systems, Faculty of Mathematics and Natural Sciences, Institut Teknologi Bandung, Jalan Ganesa 10 Bandung 40132, Indonesia
[2]Department of Nautica, Cirebon Maritime Academy, Jalan Dukuh Semar 1, Kecapi, Harjamukti, Cirebon 45142, Indonesia
[3]Physics Education, Faculty of Teacher Training and Education, University of Flores, Jalan Sam Ratulangi, Paupire, Ende Tengah, Ende, East Nusa Tenggara 86316, Indonesia
[4]Center for Mineral, Coal and Geothermal Resources, Geological Agency, Ministry of Energy and Mineral Resources of Indonesia, Jalan Soekarno-Hatta 444 Bandung 40254 Indonesia
[5]Geophysics, Faculty of Mathematics and Natural Sciences, Universitas Padjadjaran, Jalan Raya Bandung – Sumedang Km 21, Jatinangor, Sumedang 46353, Indonesia
[6]Agency for Meteorology Climatology and Geophysics (BMKG), Jalan Cemara 66, Bandung 40161, Indonesia
[7]Geophysical Engineering, Faculty of Mining and Petroleum Engineering, Institut Teknologi Bandung, Jalan Ganesa 10 Bandung 40132, Indonesia
*E-mail: wahyu@fi.itb.ac.id

Highlights:

- Spectral analysis of ground magnetic data recorded at Lesugolo area, Flores Island, Indonesia was implemented.
- The resulting Curie point depth map can be explained by the tectonic setting beneath Flores Island formed by a subducting oceanic plate, a forearc sliver, a partial melt zone, and a magma chamber.
- The thermal gradient and heat flow maps derived mathematically from the Curie point depth map provide supporting information for delineating the Lesugolo geothermal prospect area.

Abstract. The Curie point depth, or magnetic basal depth, of the Lesugolo geothermal area in Ende, Flores Island, East Nusa Tenggara, Indonesia was estimated by performing spectral analysis on spatial magnetic data and transforming it into the frequency domain, resulting in a link between the 2D spectrum of magnetic anomalies and the depths of the top and centroid of the magnetic sources. Shallow Curie point depths of 16 to 18 km were found in the north-northeast to southeast areas of Lesugolo, while deeper depths of 24 to 26 km were found in the southwest. The tectonic setting beneath the central part of Flores Island governs the distribution of the Curie point depths in the area. Shallow Curie

Received December 29th, 2020, Revised May 12th, 2021, Accepted for publication July 8th, 2021.
 ISSN: 2337-5779,
DOI: 10.5614/j.eng.technol.sci.2022.54.1.11

point depth zones are associated with high thermal gradients (30 to 34 °C/km) and heat flow (80 to 100 mW/m^2). Deep depths, on the other hand, correspond to zones of low thermal gradient (21 to 26 °C/km) and low heat flow (65 to 80 mW/m^2). Both the derived thermal gradient and the heat flow maps contribute to a better understanding of the Lesugolo geothermal system's configuration. This study suggests that the Lesugolo geothermal area's prospect zone is located in the center of the investigated area, where the Lesugolo normal fault forms its southeastern boundary.

Keywords: *Curie point depth; Flores Island; geothermal system of Lesugolo; ground magnetic data; spectral analysis.*

1 Introduction

The Curie point depth is the depth where the dominant magnetic minerals in the crust change from a ferromagnetic state to a paramagnetic state due to the influence of increasing temperature [1] so that the ability to detect magnetic anomalies above the Curie temperature disappears. The deepest layer of magnetic material in the crust is interpreted as the depth of the Curie point. The term Curie point depth is used to describe the estimated depth of magnetization contrast from magnetic anomalies at the depth of the Curie transition, which has a range of up to tens of kilometers below the earth's surface [2].

All magnetic anomalies are caused by rocks superimposed on the earth's magnetic field or the main magnetic field so that there is a change in the total magnetic field [3]. In practice, magnetic field anomalies are described as the difference between the magnetic field and the Earth's magnetic field (IGRF – International Geomagnetic Reference Field) [4], where those magnetic anomalies are caused by magnetization contrasts of rocks with different magnetic properties that are in close proximity to one another. To obtain magnetic anomalies from the total magnetic field, it is necessary to do IGRF correction and diurnal correction due to the influence of the external magnetic field.

Spectral analysis can be used to relate the spectrum of data with the depth position of a particular source object. In this study, spectral analysis was used to estimate the depth of a basement in terms of the Curie depth. The objective of this study was to apply spectral analysis to magnetic data from the Lesugolo area, Flores Island, East Nusa Tenggara, Indonesia to obtain the Curie point depth. The information about the Curie point depth can then be used for determining the thermal gradient and heat flow for the estimation of the geothermal potential of the area.

2 Geological Setting

The Lesugolo area is located at 8°32’00" to 8°38’00" S and 121°50’30" to 121°56’30" E. Geothermal manifestations at Lesugolo take the form of hot springs with neutral pH in two locations, namely: Lesugolo hot spring (94 to 98 °C) and Ae Dhara hot spring (77 °C). The Lesugolo area is divided into three groups of geomorphological units with an altitude between 25 and 1150 m. An old caldera occupies the north-northwest part of Lesugolo and is composed of Quaternary volcanic rocks in the form of pyroclastic flows and lava. Wavy hills stretch northeast-southwest and occupy the southern area, which is composed of volcanic sedimentary rocks in the form of tuff, tuff breccia, and some limestone. Alluvial plains occupy areas along the Ndondo river in the northeast that are composed of loose material from tuffs, breccias, andesite, and other mineralized rocks.

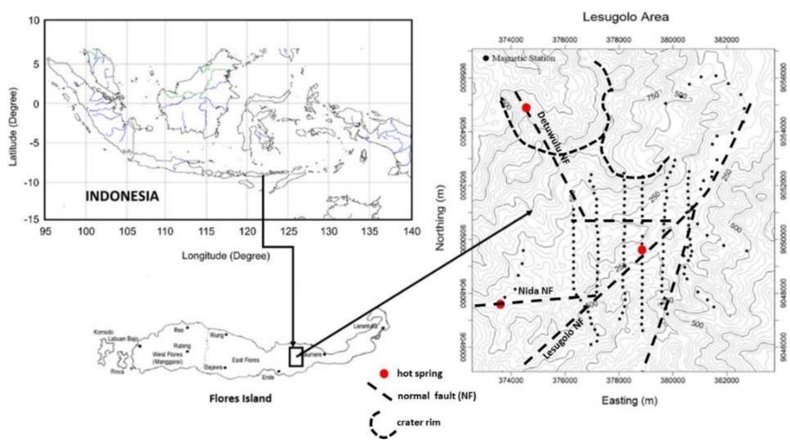

Figure 1 Map of the study area. Lesugolo is located in the province of East Nusa Tenggara, Indonesia.

The Lesugolo stratigraphy is grouped into ten rock units, namely: tuff breccia, tuff, andesitic intrusion, dacitic intrusion, limestone, Watuapi lava flow rock, Wolopelo lava flow rock, Wolopelo pyroclastic flow rock, landslide deposits, and alluvium. The tuff breccia is the oldest unit of the Lower Miocene Kiro formation, while the alluvium is the youngest unit in the Holocene-Resen age.

There are five normal faults in the Lesugolo area. The Lesugolo Fault is directed northeast-southwest and controls the appearance of the Lesugolo hot springs. The Nida Fault, which controls the emergence of the Ae Dhara hot springs, has an almost west-east trend. The Wea Fault is west-east trending with an inclination towards the north. The Detuwulu Fault runs almost northwest-southeast and controls the emergence of the Ae Petu and Lowo Geru hot springs. The Lise Fault is relatively northeast-southwest trending. The fluid of the Lesugolo geothermal system comes from meteoric water flowing into reservoir rock in the form of tuff and tertiary breccias as well as quaternary pyroclastic flows.

3 Ground Magnetic Data

The magnetic data used were obtained from an integrated investigation of the geothermal area of Lesugolo, Ende Regency, Flores Island, East Nusa Tenggara by the Center for Mineral, Coal and Geothermal Resources (PSDMBP) of the Ministry of Energy and Mineral Resources of Indonesia. The field data collection took place in August 2002. Measurements were made with a distance between measuring points of 250 m, and the total area was 10 km x 10 km (Figure 1). The ground magnetic data, in the form of magnetic field intensity (in nT), were recorded using two proton precession magnetometers. Proton precession magnetometers work on the principle that protons rotate on an axis associated with a magnetic field in all atoms.

Protons tend to naturally line up with the magnetic field of the earth. The protons will align themselves with a new field when they are exposed to an artificially induced magnetic field. The protons return to their original alignment with the magnetic field of the earth as this new field disappears. The spinning protons precede as they modify their orientation, mimicking a gyroscopic movement. The frequency of the proton precession is directly proportional to the strength of the magnetic field [3-5]. One magnetometer was fixed at a base station measuring the values of magnetic diurnal variation, which, together with the IGRF values, should be corrected to the data at all observation stations (Fig. 1) measured by the other magnetometer. The corrected magnetic data are usually called the total magnetic anomalies.

4 Method

The Curie point depth was estimated by performing spectral analysis on magnetic data. The basis of 2D spectral analysis has been described by Spector & Grant [6]. They estimated the Curie depth as the depth of a magnetized prism (z_t) obtained from the logarithmic slope of the power spectrum. Bhattacharyya & Leu [7,8] utilized this information to calculate the centroid depth of the magnetic source bodies (z_0). Okubo [2] reformulated the magnetic anomaly spectrum from Spector & Grant [6], which showed that the model's expected spectrum is the same as a single object with the average parameters from a collection of objects. The spectrum represented by polar coordinates (r, θ) in frequency space has the following form [2,9]:

$$\begin{aligned} F(r,\theta) = 2\pi JA[N + i(L\cos\theta + M\sin\theta)] \\ \times \left[n + i(\ell\cos\theta + m\ \sin\theta)\right] \\ \times \text{sinc}\ (\pi ra\ \cos\theta)\ \text{sinc}\ (\pi rb\ \sin\theta) \\ \times\ \exp\ (\text{-}2\pi ri(x_0\cos\theta + y_0\sin\theta)) \\ \times[\exp\ (\text{-}2\pi rz_{\mathrm{t}}) - \exp\ (\text{-}2\pi rz_{\mathrm{b}})] \end{aligned} \tag{1}$$

where J is the magnetization per unit volume; A is the object's average cross-sectional area; L, M, N are the cosine directions of the magnetic field; l, m, n are the cosine directions of the mean magnetization vector; a and b are the average dimensions of the object in the x and y directions; x_0 and y_0 are the means of the x and y centers. z_t and z_b are the average depths of the object's upper and lower bounds. r is the wavenumber divided by 2π or $r = k/2\pi$.

Estimation of the depth of the lower bound z_b is carried out in two steps [7,8]. The first step is to estimate the depth of the centroid z_0 with x_0 and y_0 as the coordinates of the center of the magnetic source. The second step is to determine z_t as the top depth. The bottom depth (basal depth) z_b, which is summarized as the depth of the Curie point, is calculated with the following equation:

$$z_b = 2z_0 - z_t\ . \tag{2}$$

4.1 Obtaining z_0

Here we introduce a new parameter, z_0, to rearrange the spectrum into the hyperbolic sine function z_t and z_b plus the centroid portion. At long wavelengths, the hyperbolic sine tends to be 1 and leaves a single part containing the z_0 or centroid so that the depth of the centroid is obtained with the following approximate spectrum expression [9]:

$$\begin{aligned} F(r,\theta) = 4\pi^2 VJr[N + i(L\cos\theta + M\sin\theta)] \\ \times\ \left[n\ +\ i(\ell\cos\theta + m\ \sin\theta)\right] \\ \times\ \exp\ (\text{-}2\pi ri(x_0\cos\theta + y_0\sin\theta)) \\ \times[\exp\ (\text{-}2\pi rz_0) \end{aligned} \tag{3}$$

where V is the average volume of the object. For the dipole spectrum, Eq. (3) can be modified as follows [7]:

$$G(r,\theta) = \frac{1}{r}F(r,\theta)\,. \tag{4}$$

Referring to the estimation method [6,10], the average radial power spectrum is obtained by squaring the amplitude $G(r, \theta)$ in the frequency domain [2]:

$$H^2(r) = \frac{1}{2\pi}\int_{-\pi}^{\pi}\left|G(r,\theta)^2\right|d\psi \,, \tag{5}$$

where H then can be written as:

$$\begin{aligned} H(r) &= B\exp(-2\pi r z_0) \\ \ln H(r) &= \ln B - 2\pi r z_0 \end{aligned} . \tag{6}$$

The depth of the centroid z_0 can be estimated from ln $H(r)$ using least-square fitting. By defining $P(r)$ as the mean of the radial power spectrum $H^2(r)$, Eq. (6) can be rewritten as:

$$\ln\left[\frac{P(r)^{1/2}}{|r|}\right] = \ln A - 2\pi|r|z_0 \,. \tag{7}$$

where r is the wavenumber and B is a constant.

4.2 Obtaining z_t

The estimated depth of the upper limit z_t can be obtained by utilizing the slope of the spectrum with the second-longest wavelength. The resulting spectrum approximation is

$$\begin{aligned} F(r,\theta) = 2\pi^2 VJ[N + i(L\cos\theta + M\sin\theta)] \\ \times\ [n + i(\ell\cos\theta + m\ \sin\theta)] \\ \times\ \exp(-2\pi ri(x_0\cos\theta + y_0\sin\theta)) \,. \\ \times[\exp(-2\pi r z_t) \end{aligned} \tag{8}$$

This spectrum only differs by r from the z_0 spectrum because the z_t spectrum is a monopole spectrum. In the same way as in the first step, the mean radial power spectrum is obtained as follows [2]:

$$K^2(r) = \frac{1}{2\pi}\int_{-\pi}^{\pi}\left|F(r,\theta)\right|^2 d\psi \,. \tag{9}$$

If we only consider the depth factor, the approximation of the above equation is as follows:

$$\begin{aligned} K(r) &= C \exp(-2\pi r z_t) \\ \ln K(r) &= \ln C - 2\pi r z_t \end{aligned} \tag{10}$$

where C is a constant.

The solution of the magnetic anomaly spectrum produces a linear equation that indicates the depth of the lower boundary of the magnetized object. To ensure the linearity of the equation it is necessary to transform anomalies from the spatial domain to the frequency domain. The effect of the lower bound of the magnetized body is mostly concentrated at the lower frequencies of the spectrum. Domain transformation is needed to clarify the effect of low frequency compared to high frequency [11].

By defining *P(r)* as the mean of the radial power spectrum *K2(r)*, we obtain:

$$\ln\left[P(r)^{1/2}\right] = \ln C - 2\pi|r|z_t \tag{11}$$

where C is a constant. The basal depth of z_b can then be obtained from magnetic sources by

$$z_b = 2z_0 - z_t \tag{12}$$

basal depth z_b from the magnetic source from Eq. (12) is inferred as the depth of the Curie point.

The geothermal gradient between the earth's surface and the Curie point depth z_b expressed in Curie temperature θ_C is given by [12-14]:

$$\frac{dT}{dZ} = \frac{\theta_C}{z_b}, \tag{13}$$

where θ_C equals 580 °C.

The heat flow and the thermal gradient of an area can be calculated using Fourier's law [12,15] with the following formula:

$$Q = \lambda\left(\frac{dT}{dZ}\right) = \lambda\left(\frac{580°\mathrm{C}}{z_b}\right) \tag{14}$$

where Q is the heat flow and λ is the heat conductivity, which is 2.5 W/mK as the average value of the igneous rock above the basement. From this equation, it can be seen that the Curie depth point is inversely proportional to the heat flow.

5 Results and Discussion

The magnetic anomaly data obtained from the field are diurnal variation and IGRF corrected prior to further processing. The corrected magnetic anomaly values were predominantly in the range of -80 to 60 nT (Figure 2(a)). There were pairs of low and high anomaly values in the eastern part of the study area, with low values reaching -220 nT and high values reaching 340 nT. There were also low anomalous values in the southwest part of the study area.

The total magnetic anomaly map cannot be interpreted directly because the magnetic dipole system causes the anomaly to not be directly above the causative body. The reduction to pole process (RTP) was carried out by mathematically rotating the inclination direction of 90° and declination of 0° so that the anomaly is right above the causative body, assuming that the magnetic remanence is very small compared to the magnetic induction. On the RTP map (Figure 2(c)) there is a pair of high (400 nT) and low (-400 nT) anomaly patterns in the eastern part of the study area.

The next step was the application of the upward continuation technique to the RTP data to eliminate the effects of local anomalies and topography so that the magnetic anomalies were valid in reflecting the deeper crustal magnetic source. The RTP and upward continuation processes produce an optimum anomaly map at an altitude of 500 meters. On the magnetic anomaly map resulting from the upward continuation (Figure 2(d)), the negative anomaly in the eastern part is more clearly visible. This magnetic anomaly map was then used in determining the Curie point depth.

5.1 Shallow Geothermal System

Before proceeding with the spectral analysis, it is worthwhile to notice based on features shown in Figure 3 that moderately low to low magnetic anomalies were found along the Lesugolo normal fault and another fault in the southeastern part of the investigated area. This feature may be attributed to the lessening of the magnetization of rocks at a relatively shallow crust, which can be elucidated by the loss of magnetic properties at high temperatures or by chemical alterations affecting magnetic minerals and hydrothermal fluid circulation inside the rocks [16-19]. PSDMBP [20] reported that high gravity anomalies are concentrated in zones that coincide with Blocks 8 and 11, which is interpreted as being due to the presence of intrusive andesite. If this is true, then the intrusive body should be hot enough to cause the rocks to undergo demagnetization due to hydrothermal alteration. The evidence of low apparent resistivity values (< 20 ohm.m) measured by DC resistivity sounding with AB/2 = 1000 was also reported in [20] covering Blocks 7 and 8, including the Lesugolo hot spring. This low resistivity zone may indicate the presence of impermeable hydrothermally altered rocks potentially overlying a potential geothermal reservoir [21].

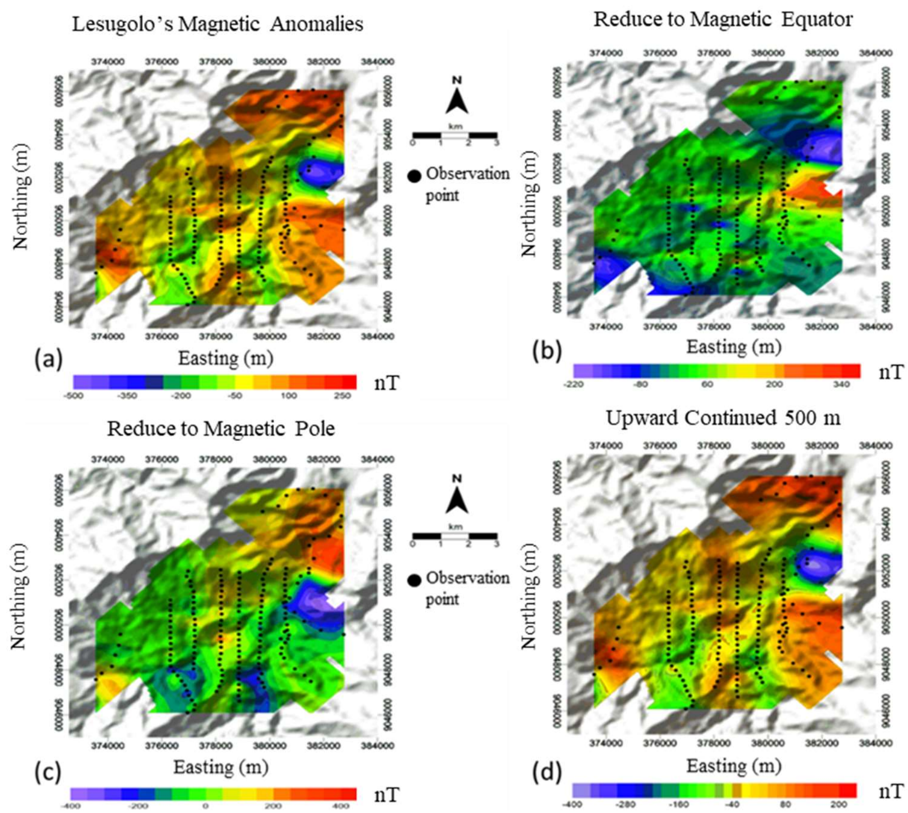

Figure 2 (a) Magnetic anomaly data, (b) output from RTE, (c) output from RTP and (d) 500-meter upward continuation of RTP.

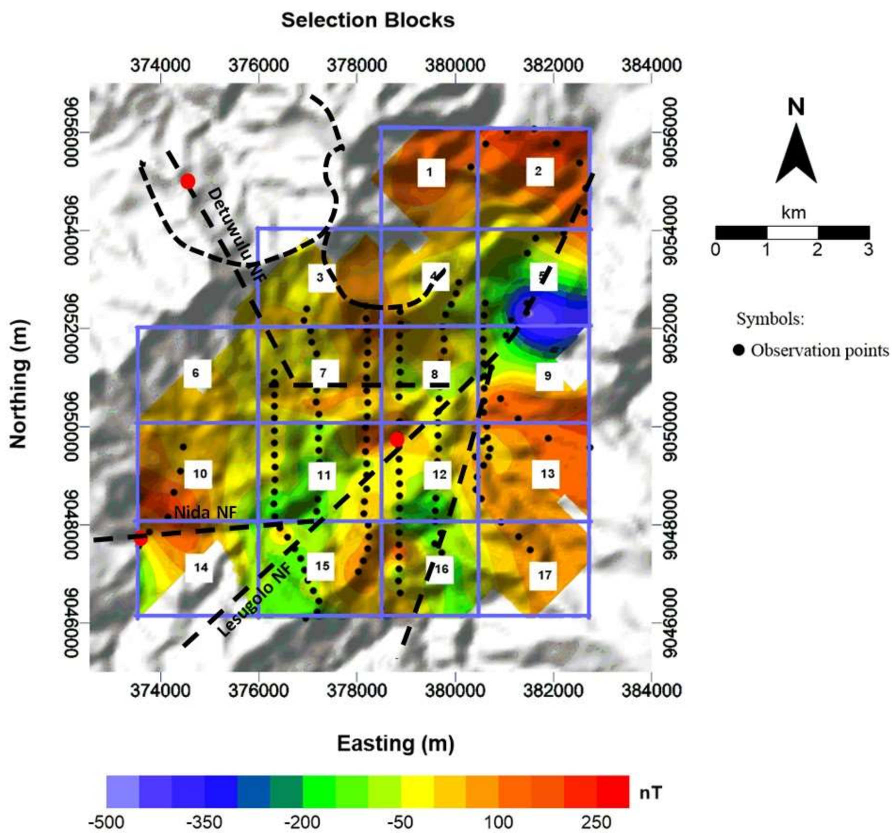

Figure 3 The study area was divided into 17 blocks with varying sizes between 2 km x 2 km and 2.5 km x 2.5 km. Within each block, a grid of 100 m was formed.

In geothermal systems, mercury (Hg) exists as a result of the absorption of vapor and volcanic gasses into thermal waters, and upon migrating to the surface, together with CO_2 and H_2S, Hg can be accumulated in soils [22,23]. A high concentration of soil Hg of about 200 to 400 ppb was reported by PSDMBP [20] along the Lesugolo normal fault in coincidence with zones covered by Blocks 8, 11, 12, and 15. A high concentration of soil Hg on the surface is an indicator of an upflow zone with a geothermal reservoir lying beneath. Considering all the available geological, geochemical and geological evidence, it is likely that the geothermal system in the shallow part of the Lesugolo area is a type of fault-controlled geothermal system.

5.2 Curie Point Depths

For the sake of Curie point depth analysis, the study area was divided into 17 blocks (Figure 3). The Curie point depth in each block was then estimated to obtain the distribution of the magnetic basement depth in the Lesugolo area. The dimensions of the blocks vary in size from 2 km x 2 km to 2.5 km x 2.5 km. Each one of the blocks contains vertical and horizontal grids at a distance of 100 m.

The magnetic anomaly data was transformed into the frequency domain using the 2D Fourier transform to obtain the average radial power spectrum for calculating z_0, z_b, and z_t. Figure 4 shows an example of extracting depth values for z_0 and z_t in Block 5 (Figure 4(a)) and Block 7 (Figure 4(b)). On these two blocks, data distribution with a linear trend was selected in areas with small wavenumber values. Then the data was fitted with a straight line so that the slope of the line was obtained, showing the depth values of z_0 and z_t. From the z_0 and z_t depth values, the z_b depth distribution could be obtained, which is defined as the depth of the Curie point where materials change their magnetic properties due to the heating system beneath them.

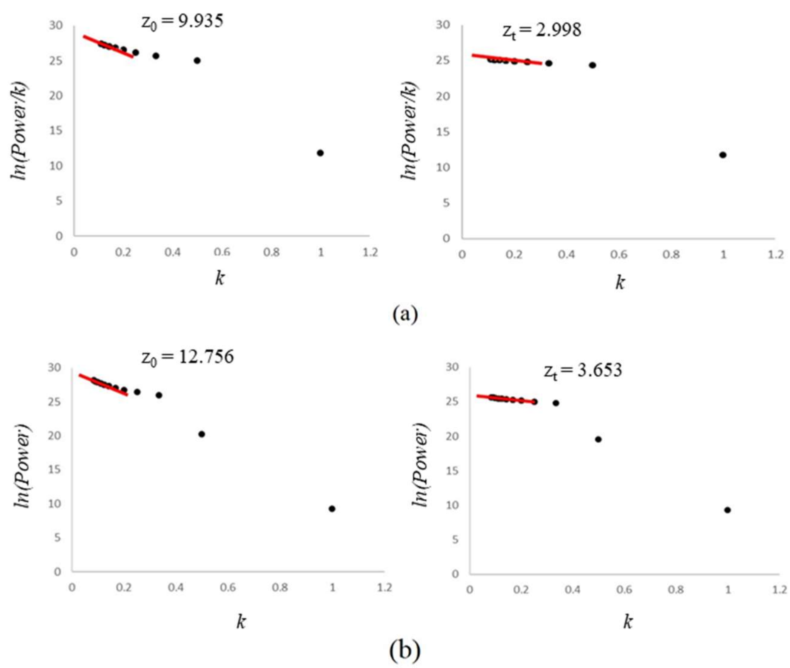

Figure 4 Calculation of z_0 and z_t from a) Block 5 and b) Block 7.

In Block 5, the centroid and basal depths were z_0 = 9.93 km and z_t = 2.99 km, so that the Curie depth z_b was 16.88. In Block 7 it was found that z_0 = 12.76 km and z_t = 3.65 km, and the Curie point depth z_b was 21.86. The calculated Curie point depths are listed in Table 1. The average value of the Curie point depths was about 20 km with a shallowest depth of 16 km and a deepest depth of 26 km (Figure 5(a)). A distribution map of gradient thermal and heat flow in the Lesugolo area was then calculated from the estimated Curie point depths.

From the Curie point depth map depicted in Figure 5(a), deeper Curie point depths of about 24 to 26 km are situated in the southwestern area, while shallower Curie point depths of about 16 to 18 km extend from the north-northeast to southeast areas (Figure 5(a)). These shallower Curie point zones may have a strong contribution to the heating system beneath the shallow Lesugolo geothermal area, predominantly in the form of magmatism. The newest cross-section 3D seismic P-wave velocity model of the Lesugolo area in the N-S direction, from the current study, is shown in Figure 6.

Table 1 Curie depth, thermal gradient, and heat flow values for each block.

Block Number	Depth to Centroid Z_0 (km)	Depth to Top Z_t (km)	Depth Curie Point Z_b (km)	Thermal gradient (°C/km)	Heat flow (mW/m²)
1	10.97	2.56	19.37	29.94	89.16
2	10.97	3.71	18.23	31.81	94.74
3	10.97	1.78	20.15	28.78	85.70
4	10.97	2.99	18.95	30.61	91.15
5	9.93	2.99	16.88	34.36	102.32
6	10.97	2.14	19.80	29.29	87.23
7	12.76	3.65	21.86	26.53	79.02
8	9.93	2.56	17.30	33.52	99.81
9	11.91	1.78	22.04	26.31	78.35
10	11.91	2.17	21.69	26.74	79.63
11	14.85	3.20	26.50	21.89	65.18
12	11.91	3.71	20.12	28.82	85.84
13	11.91	4.02	19.81	29.28	87.19
14	9.93	2.14	17.73	32.71	97.40
15	13.84	3.20	24.49	23.69	70.54
16	10.97	3.37	18.57	31.23	93.00
17	11.91	3.37	20.46	28.34	84.41
Mean	11.57	2.90	20.23	29.05	86.51
Min	9.93	1.78	16.88	21.89	65.18
Max	14.85	4.02	26.50	34.36	102.32

The high V_P zones in Figure 6 represent the denser Australian oceanic lithosphere, which is subducting beneath the lighter Eurasian plate and the forearc sliver beneath Flores Island's volcanic arc [24], which includes the Lesogolo area. The presence of a low V_P zone (down to about -25 km) representing a magma chamber and another zone at about -80 to -120 km representing a partial melting zone beneath the central-north part of the traversed Flores Island provide a strong explanation of why the Curie point depths are shallower in the northern part of the Lesugolo area, in contrast to its south-southwestern part, which lays above a thin magma-related low V_P zone and a forearc sliver.

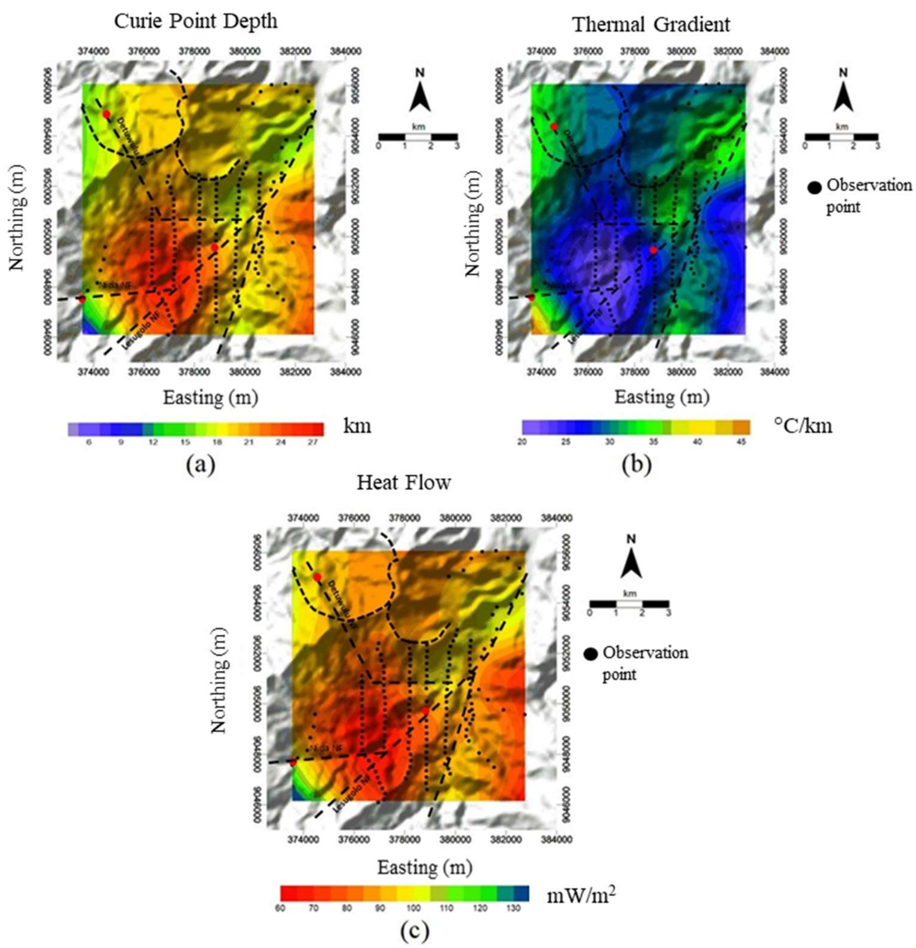

Figure 5 (a) Curie depth, (b) thermal gradient, and (c) heat flow in the study area.

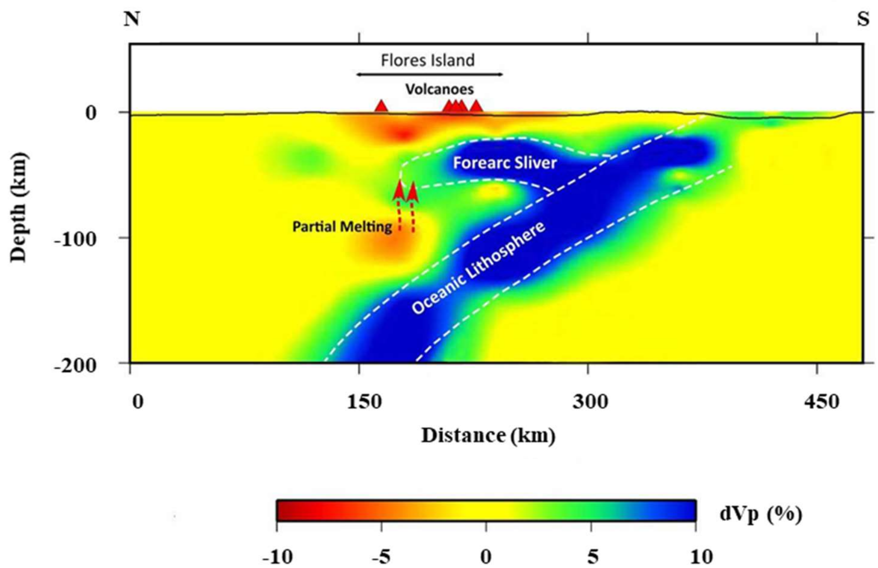

Figure 6 N-S cross-section of 3D seismic P-wave velocity model traversing the central part of Flores Island.

As a consequence of Eqs. (13) and (14), the estimated thermal gradient and heat flow maps of the investigated area are inversely proportional to the Curie point depth map, respectively. The thermal gradient map (Figure 5b) shows that a high thermal gradient of 30 to 34 °C/km extends from the northeastern-central to the southeastern areas, which is strongly correlated with the shallow zones of Curie point depth. In the same high thermal gradient zones, high heat flow values of 80 to 100 mW/m^2 can be observed. Meanwhile, low thermal gradient zones of 21 to 26 °C/km correlate with low heat flow zones of 65 to 80 mW/m^2. The temperature of the hot spring located at the center of the investigated area (Lesugolo hot spring) is 94.5 °C, whereas the temperature of the hot spring located in the southwest of the investigated area (Ae Dhara hot spring) is 72.45 °C [20].

Both hot springs are situated at the boundary between high and thermal gradient zones. The estimated reservoir temperatures calculated based on Na/K fluid geothermometry for both hot springs are 197 °C and 187 °C, respectively. These features are consistent with the thermal gradient and heat flow maps, which suggest higher thermal activity in the northeastern-central part of the investigated area. From a practical perspective, considering the necessity of determining a geothermal prospect zone at Lesugolo area and taking into account all the information presented from this study and from previous works, it is likely that the prospective upflow zone, where the geothermal reservoir is located, is the area covered by Block 8, with Lesugolo hot spring being on the outflow zone.

6 Conclusion

Curie point depth estimation was successfully performed on ground magnetic data measured at Lesogolo geothermal area, Ende, Flores Island, East Nusa Tenggara, Indonesia, covering an area of 10 km x 10 km. The depths of the magnetic source's upper bounds and centroids were extracted from the spectral data curves, which in turn yielded the estimated Curie point depths. Shallow Curie point depths of 16 to 18 km extend from the north-northeastern to the southeastern parts of Lesugolo, and deeper Curie point depths of 24 to 26 km are concentrated in the southwestern part. These features may be attributed to the N-S tectonic setting beneath the center part of Flores Island, where a relatively thick magma chamber and a deeper partial melt zone exist. The derived thermal gradient and heat flow maps also confirmed several indications of the Lesugolo geothermal system based on geological features and other geophysical and geochemical surveys.

Acknowledgement

This study was partially funded by Research, Community Service, and Innovation Program (P3MI), Institute of Research and Community Service (LPPM) ITB contract no. 541E/I1.C01/PL/2020.

References

[1] Nagata, T., *Rock Magnetism*, Maruzen: Tokyo, 1961.
[2] Okubo, Y., Graf, R.J, Hansen, R.O, Ogawa, K. & Tsu, H., *Curie Point Depths of Island of Kyushu and Surrounding Areas*, Japan, Geophysics, **53**, pp. 481-494, 1985.
[3] Kaerey, P., Brooks, M. & Hill, I., *An Introduction to Geophysical Exploration*, Blackwell Science: UK, 2002.
[4] Lowrie, W., *Fundamental of Geophysics*, Cambridge university press: New York, 2007.
[5] John M. & Asger E. *Field Geophysics*, 4th ed., John Wiley & Sons Ltd., West Sussex, PO19 8SQ, United Kingdom, 2011.
[6] Spector, A. & Grant, F.S., *Statistical Models for Interpreting Aeromagnetic Data*, Geophysics, **35**, pp. 293-302, 1970.
[7] Bhattacharyya, B.K. & Leu, L.K., *Spectral Analysis of Gravity and Magnetic Anomalies Due to Two-Dimensional Structures*, Geophysics, **40**, pp. 993-1013, 1975.

[8] Bhattacharyya, B.K. & Leu, L.K., *Analysis of Magnetic Anomalies over Yellowstone National Park: Mapping of Curie Point Isothermal Surface for Geothermal Reconnaissance*, Journal of Geophysical Research, **80**, pp. 4461-4465, 1975.
[9] Dolmaz, M.N., Hisarli, Z.M., Ustaömer, T. & Orbay, N., *Curie Point Depths Based on Spectrum Analysis of Aeromagnetic Data*, West Anatolian Extensional Province, Turkey, Pure Appl. Geophys., **162**, pp. 571-590, 2005.
[10] Shuey, R.T, Schellinger, D.K, Tripp, A.C. & Nley, L.B., *Curie Depth Determination from Aeromagnetic Spectra*, Geophys. J. R. Astr. Soc, **50**, pp. 75-101, 1977.
[11] Bhattacharyya, B.K. & Leu, L.K., *Spectral Analysis of Gravity and Magnetic Anomalies due to Rectangular Prismatic Bodies*, Geophysics, **42**, pp. 41-50, 1977.
[12] Tanaka. A. Okubo, Y. & Matsubayasi, O., *Curie Point Depth Based on Spectrum Analysis of the Magnetic Anomaly Data in East and Southeast Asia*, Tectonophysics, **306**, pp. 461-470, 1999.
[13] Stampolidis, A., Kane, I., Tsokas, G.N., & Tsourlos, P., *Curie Point Depths of Albania Inferred from Ground Total Field Magnetic Data*, Surveys in Geophysics, **26**, pp. 461-480, 2005.
[14] Maden, N., *Curie-Point Depth from Spectral Analysis of Magnetic Data in Erciyes Stratovolcano (Central TURKEY)*, Pure Appl. Geophys., **167**, pp. 349-358, 2010.
[15] Turcotte, D.L. & Schubert, G., *Geodynamics,* Cambridge University Press, New York, 1982.
[16] Blanco, I., García, A. & Torta, J.M., *Magnetic Study of the Furnas Caldera (Azores).*, Ann. Geophys., **40**, pp. 341-359, 1997.
[17] Hochstein, M.P. & Soengkono, S., *Magnetic Anomalies Associated with High Temperature Reservoirs in The Taupo Volcanic Zone (New Zealand)*, Geothermics, **26**, pp. 1-24, 1997.
[18] Caratori T.F., de Ronde, C.E.J. Scott, B.J., Soengkono, S., Stagpoole, V., Timm, C. & Tivey, M, *Interpretation of Gravity and Magnetic Anomalies at Lake Rotomahana: Geological and hydrothermal implications*, J. Volcanol. Geoth. Res., **314**, pp. 84-94, 2016.
[19] Paoletti, V., Passaro, S., Fedi, M., Marino, C., Tamburrino, S. & Ventura, G., *Sub-Circular Conduits and Dikes Offshore the Somma-Vesuvius Volcano Revealed by Magnetic and Seismic Data*, Geophys. Res. Lett., **43**, pp. 9544-9551, 2016.
[20] Center for Mineral Resources, Coal, and Geothermal (PSMBPBG), Geological Agency of Indonesia & Directorate of New and Renewable Energy and Energy Conversion, *Geothermal Potency of Indonesia, 2nd Book*, Ministry of Energy and Mineral Resources of Indonesia, 2017. (Text in Indonesian)

[21] Pellerin, L., Johnson, J.M. & Hohmann, G.W., *A Numerical Evaluation of Electromagnetic Methods in Geothermal Exploration*, Geophysics, **61**(1), pp. 121-130, January-February 1996.

[22] Herdianita, N.R. & Priadi, B., *Arsenic and Mercury Concentrations at Several Geothermal Systems in West Java*, Indonesia, J. Sci. **40A**(1), pp. 1-14, 2008.

[23] Rychagov S.N., Nuzhdaev, A.A. & Stepanov, I.I., *Mercury as an Indicator of Temperature and Geochemical Barriers in Hypergenesis Zone of Geothermal Deposits (Kamchatka)*, Proceedings World Geothermal Congress 2010 Bali, Indonesia, **1**, pp. 25-29 April 2010

[24] Supendi, P., Nugraha, A.D., Widiyantoro, S., Abdullah, C.I., Rawlinson, N., Cummins, P.R., Harris, C.W., Roosmawati, N. & Miller, M.S., *Fate of Forearc Lithosphere at Arc-Continent Collision Zones: Evidence from Local Earthquake Tomography of the Sunda-Banda Arc Transition*, Indonesia. Geophysical Research Letters, **47**, pp. 1-9, 2020.